Atmospheric
Measurement
Techniques

A versatile, refrigerant- and cryogen-free cryofocusing–thermodesorption unit for preconcentration of traces gases in air

Florian Obersteiner[1], Harald Bönisch[2], Timo Keber[1], Simon O'Doherty[3], and Andreas Engel[1]

[1]Institute for Atmospheric and Environmental Science, Goethe University Frankfurt, Frankfurt, Germany
[2]Institute of Meteorology and Climate Research, KIT, Karlsruhe, Germany
[3]School of Chemistry, University of Bristol, Bristol, UK

Correspondence to: Florian Obersteiner (obersteiner@iau.uni-frankfurt.de)

Abstract. We present a compact and versatile cryofocusing–thermodesorption unit, which we developed for quantitative analysis of halogenated trace gases in ambient air. Possible applications include aircraft-based in situ measurements, in situ monitoring and laboratory operation for the analysis of flask samples. Analytes are trapped on adsorptive material cooled by a Stirling cooler to low temperatures (e.g. $-80\,^\circ$C) and subsequently desorbed by rapid heating of the adsorptive material (e.g. $+200\,^\circ$C). The set-up involves neither the exchange of adsorption tubes nor any further condensation or refocusing steps. No moving parts are used that would require vacuum insulation. This allows for a simple and robust design. Reliable operation is ensured by the Stirling cooler, which neither contains a liquid refrigerant nor requires refilling a cryogen. At the same time, it allows for significantly lower adsorption temperatures compared to commonly used Peltier elements. We use gas chromatography – mass spectrometry (GC–MS) for separation and detection of the preconcentrated analytes after splitless injection. A substance boiling point range of approximately -80 to $+150\,^\circ$C and a substance mixing ratio range of less than 1 ppt (pmol mol^{-1}) to more than 500 ppt in preconcentrated sample volumes of 0.1 to 10 L of ambient air is covered, depending on the application and its analytical demands. We present the instrumental design of the preconcentration unit and demonstrate capabilities and performance through the examination of analyte breakthrough during adsorption, repeatability of desorption and analyte residues in blank tests. Examples of application are taken from the analysis of flask samples collected at Mace

Head Atmospheric Research Station in Ireland using our laboratory GC–MS instruments and by data obtained during a research flight with our in situ aircraft instrument GhOST-MS (Gas chromatograph for the Observation of Tracers – coupled with a Mass Spectrometer).

1 Introduction

Atmospheric trace gases introduced to or elevated in concentration in the environment by human activities often show adverse environmental impacts. Prominent examples are chlorofluorocarbons (CFCs) and their intermediate replacements, and hydrochlorofluorocarbons (HCFCs), which deplete stratospheric ozone (Farman et al., 1985; Molina and Rowland, 1974; Montzka et al., 2011; Solomon, 1999). Present-day CFC replacements, namely hydrofluorocarbons (HFCs), have zero ozone depletion potentials (ODPs) but are still potent greenhouse gases like CFCs and HCFCs (Hodnebrog et al., 2013; Velders et al., 2009). Another example is non-methane hydrocarbons (NMHCs), which produce harmful tropospheric ozone in the presence of nitrogen oxides (Haagen-Smit and Fox, 1956; Marenco et al., 1994; Monks et al., 2015).

Many of the species found in the compound classes named above show atmospheric concentrations too low for immediate detection and quantification by means of instrumental analytics. A preconcentration step is required. The method of cryofocusing–thermodesorption is a common technique

for that purpose (e.g. Aragón et al., 2000; Demeestere et al., 2007; Dettmer and Engewald, 2003; Eyer et al., 2016; Hou et al., 2006). In principal, an ambient air sample from either a sample flask or continuous flow for online measurement is preconcentrated on adsorptive material at a specific adsorption temperature, T_A. If T_A is significantly below ambient temperature, this step is referred to as "cryofocusing" or "cryotrapping". Trapped analytes are subsequently remobilised by heating the adsorptive material to a desorption temperature T_D and flushed, e.g. onto a gas chromatographic column with a carrier gas and detected with a suitable detector.

The primary motivation for the development of the instrumentation described in this paper was halocarbon analysis in ambient air. More specifically, there were no commercial instruments available which met the requirements of remote in situ and aircraft operation: compact (as small as possible), lightweight (< 5 kg), safe containment of working fluids and preferentially cryogen- and refrigerant-free, pure electrical operation. Cryogens like liquid nitrogen (LN_2) or argon (LAr; e.g. Apel et al., 2003; Farwell et al., 1979; Helmig and Greenberg, 1994) offer large cooling capacity but are difficult to operate on board an aircraft due to safety restrictions and supply demand, e.g. when operating the aircraft from remote airports. Compression coolers (e.g. Miller et al., 2008; O'Doherty et al., 1993; Saito et al., 2010) offer less cooling capacity in terms of heat lift compared to liquid cooling agents and are relatively large in size and weight compared to widespread Peltier type cooling options (Peltier elements; e.g. de Blas et al., 2011; Simmonds et al., 1995; commercial thermodesorbers available from e.g. Markes or PerkinElmer). Peltier elements have the advantage of being very small and requiring only electrical power for cooling. However, their cooling capacity and minimum temperature cannot compete with compression- and cryogen-based coolers. Stirling coolers pose an in-between solution, well suited for maintenance-free remote operation. Like Peltier coolers, they only require electrical power, do not contain any potentially dangerous working fluids (only helium) or cryogens but have a significantly higher cooling capacity. While not being as powerful as cryogen-based coolers (LN_2, LAr), they have comparable minimum temperatures. To our knowledge, the use of Stirling coolers for similar purposes to the ones described here is rare, with few published exceptions like the preconcentration of methane by Eyer et al. (2016) or trapping CO_2 using carbon capture technology by Song et al. (2012).

The principal design of the cryofocusing–thermodesorption unit was developed for the airborne in situ instrument GhOST-MS (Gas chromatograph for the Observation of Tracers – coupled with a Mass Spectrometer; Sala et al., 2014) and successfully used during three research campaigns up to now – 2011: SHIVA (carrier aircraft: DLR FALCON), 2013: TACTS (carrier aircraft: DLR HALO), 2015/2016: PGS (carrier aircraft: DLR HALO). To extend the substance range, we then developed similar
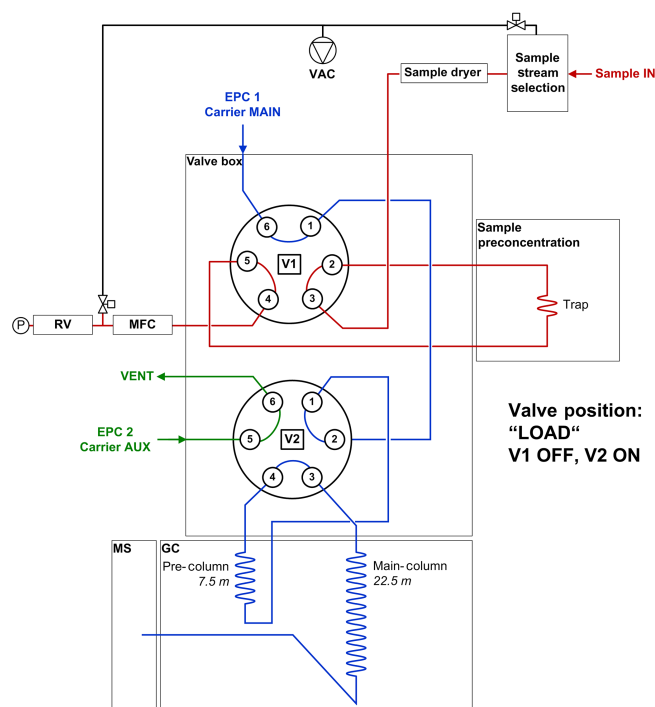

Figure 1. Flow scheme showing the gas flow during preconcentration. Two electronic pressure controllers, EPC 1 and EPC 2, control the carrier gas flow. The two 6-port 2-position rotary valves V1 and V2 are set to OFF/ON position. A sample is preconcentrated (red flow path); sample components not trapped flow through the mass flow controller (MFC) into the reference volume (RV). By switching V1 to ON position, the preconcentration trap is injected onto the GC column. The trap as well as reference volume and stream selection valves are evacuated prior to the preconcentration of the next sample. By switching V2 to OFF, it separates the pre-column and main column; the pre-column is flushed backwards. This prevents high-boiling, non-targeted species from reaching the main column.

cryofocusing–thermodesorption units for our other GC–MS (gas chromatography – mass spectrometry) instruments (Hoker et al., 2015; Obersteiner et al., 2016), which are currently operated in the laboratory. Both detailed description and characterisation of the preconcentration unit were not discussed in the publications by Hoker et al. (2015), Obersteiner et al. (2016; laboratory set-ups) and Sala et al. (2014; aircraft instrument). Within this paper, a general instrumental description is given in Sect. 2, which is applicable for all the named set-ups. Characterisation results discussed in Sect. 3. are based on the latest version of the laboratory set-up (Obersteiner et al., 2016). Only characteristics of the preconcentration set-up are discussed in this paper; instrument characteristics such as measurement precision or reproducibility can be found in the relevant publications. To demonstrate the versatility and reliability of the set-up, application examples are given in Sect. 4 for sample analysis in the laboratory as well as in situ aircraft operation. Results are summarised and conclusions are drawn in Sect. 5.

Table 1. Technical configuration of the three preconcentration set-ups. For further details on the full instruments (e.g. gas chromatography or detection), please refer to the respective references. T_D is given as a temperature range as it can be determined only indirectly (see Sect. 2.3).

Instrument	GhOST-MS (in situ)	GC-QPMS (laboratory)	GC-TOFMS (laboratory)
Reference	Sala et al. (2014)	Hoker et al. (2015)	Obersteiner et al. (2016)
Adsorptive material, type	HayeSep D, VICI, Switzerland	HayeSep D	HayeSep D (default)/Unibeads 1S, Grace, USA (testing purposes)
Adsorptive material, approx. packed volume [mm^3]	12	20	20
Stirling cooler	SC-TD08, Twinbird, Japan	M150, Global Cooling, USA (not available anymore)	CryoTel CT, Sunpower (Ametek), USA
T_A [°C], routine operation	< −70, depending on ambient temperature as cooler operates at limit	−80 (cooling capacity would allow −120)	−80 (cooling capacity would allow < −120)
T_D [°C]	180–220	180–220	180–220
reference volume [L]	2 (1 tank)	2–16 (4 tanks)	2 (1 tank)
pressure sensor	Setra 204E, Setra Systems, USA	Setra 204, Setra Systems	Baratron 626, MKS Instruments, Germany
MFC	IQ-Flow IQF-200C, Bronkhorst, the Netherlands	EL-FLOW F-201CM, Bronkhorst	EL-FLOW F-201CM
Evacuation pump	MD-1 vario SP, Vacuubrand, Germany	Trivac NT 5, Leybold (Oerlikon), Germany	MD-1 vario SP
Control/operation	LabVIEW & cRIO, National Instruments, USA	LabVIEW & cRIO	LabVIEW & cRIO

2 Implementation of cryofocusing and thermodesorption

This section gives a description of principal components of the sample preconcentration unit and is valid for all our analytical set-ups presented in Sala et al. (2014), Hoker et al. (2015) and Obersteiner et al. (2016). Technical details are listed in Table 1 for all three set-ups. The following Sect. 2.1 outlines the general measurement procedure and gas flow as well as its integration into a chromatographic detection system. Section 2.2 and 2.3 describe the implementation of the main operations of the unit: cooling ("trapping", i.e. preconcentration of analytes) and heating (desorption of analytes). The preconcentration system described was designed for coupling with a chromatographic system but, in principle, could also be adapted for coupling with other techniques.

2.1 Preconcentration procedure and integration for GC application

For the preconcentration of analytes, the sample is flushed through a micro-packed column of cooled adsorptive material. Analytes are "trapped" on the adsorptive material as the steady state of adsorption and desorption is strongly shifted towards adsorption by the low temperature of the adsorptive material. Through subsequent rapid heating of the adsorptive material, the steady state is instantaneously shifted towards desorption (thermodesorption). Formerly trapped analytes are flushed in the opposite direction to sampling flow, onto the chromatographic column with a carrier gas. The system does not involve a refocussing procedure as implemented in other preconcentration systems (e.g. Miller et al., 2008). Instead, the analytes are purged directly onto the GC col-

umn for separation. Figure 1 shows a flow scheme of the set-up. The outflow of the trap during preconcentration (stripped air; mainly nitrogen and oxygen) is collected in a previously evacuated reference volume tank for analyte quantification (2 L electro-polished stainless steel flask; volume determination by pressure difference). A mass flow controller (MFC) is mounted between the trap and reference volume for sample flow control. The MFC can also be used to determine the sample volume, thereby adding flexibility with respect to sample volumes larger than the reference tank. Hardware control is implemented with a LabVIEW cRIO assembly (compact reconfigurable input output; National Instruments Inc., USA) using custom-written control software. It operates the preconcentration unit automatically, i.e. controls system parameters like preconcentration trap temperature by cooling and heating concomitant with system states such as preconcentration and desorption.

2.2 Cryofocusing: preconcentration trap and cooling technique

A stainless steel tube with 1/16 inch outer diameter (OD) and 1 mm inner diameter (ID) is used as preconcentration trap. The tube is packed with adsorptive material and placed inside an aluminium cuboid (coldhead) which is cooled continuously to maintain a specific adsorption temperature. Figure 2 shows a technical drawing of the trap and coldhead. The coldhead can contain two traps; in this case one of them is an empty stainless steel tube with 1/16 inch OD and 1 mm ID to characterise the trap heater. For that purpose, a thin temperature sensor is inserted into the empty tube. Provided that the coldhead insulation is sufficient and intact, no significant temperature difference occurs between both traps due to the
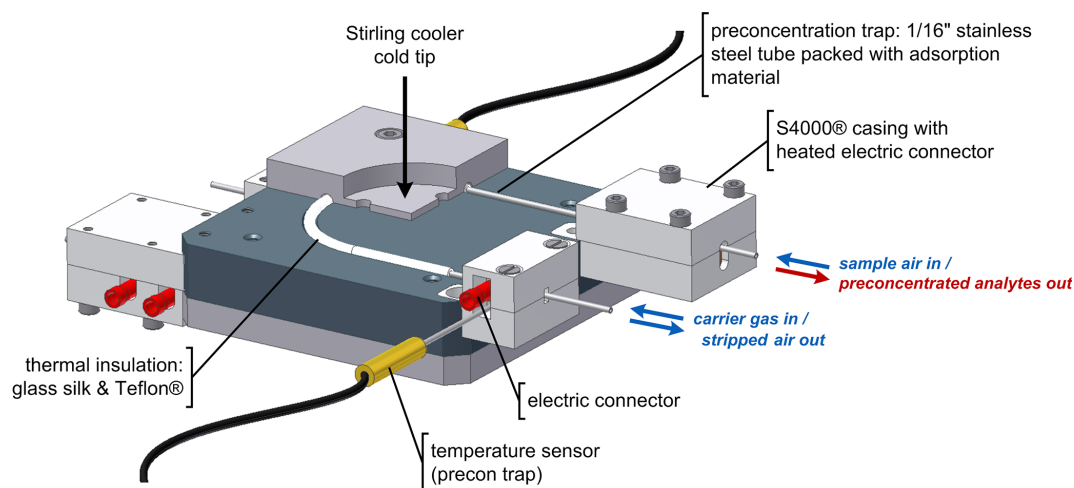
Figure 2. Technical drawing of the coldhead and preconcentration trap placed inside. Three plates of anodised aluminium can hold two traps. The Stirling cooler's cold tip screwed to the coldhead removes heat for cooling. Heat for sample desorption is generated by a current directly applied to the tubing of the trap. The electric connector in the direction of sample flow (upper right side of the drawing) is heated constantly to 150 °C to avoid a cold point due to the mass of the electric connector and its proximity to the coldhead (S4000® insulation material: Brandenburger, Germany).

high heat conductivity of the aluminium. To save space and avoid mechanical, moving parts, the preconcentration trap is not removed from the coldhead during desorption. It is insulated (and thereby isolated electrically) by two layers of glass silk and four layers of Teflon shrinking hose. The insulation is a variable parameter which determines the rate at which heat is exchanged between the trap and coldhead. Consequently, it determines coldhead warm-up rate during desorption and trap cool-down rate after desorption. More insulation would result in longer trap cool-down time after desorption but also to less heat flowing into the coldhead, thus to a lower possible temperature of the coldhead. The insulation used represents a compromise that works well for the application presented here but could potentially be improved, e.g. by using a ceramic insulator. The coldhead itself is insulated from the surrounding air with 45 mm of Aeroflex HF material (Aeroflex Europe GmbH, Germany).

The Stirling cooler used for cooling offers the advantage of requiring only electrical power while providing a relatively large cooling capacity at very low minimum temperatures. The latter are comparable to liquid nitrogen in the case of Sunpower CryoTel MT, CT and GT Stirling coolers, with maximum heat lifts of 5 to 16 W at −196 °C (77 K) according to the manufacturer. Heat that is removed from the coldhead by the Stirling cooler has to be released to the surrounding air, either directly by an air-fin heat rejection or indirectly by a water coolant system mounted to the cooler's warm side. The cooler should maintain a defined adsorption temperature T_A of the trap over the series of measurements. However, during thermodesorption, a certain amount of heat flows from the heated trap into the coldhead as the preconcentration trap is kept directly inside with only a small amount of insula-

tion. Excess heat has to be removed by the Stirling cooler to regain T_A for the preconcentration of the next sample. The preconcentration unit is attached to a gas chromatograph; therefore, the total duration of the chromatogram (chromatographic runtime) allows coldhead and trap to cool down after thermodesorption and return to T_A before preconcentrating the next sample. Besides chromatographic runtime, various factors determine the minimum cycle time (i.e. sample measurement frequency):

– sample preconcentration (volume of the sample to preconcentrate and preconcentration flow),

– sample desorption (duration and T_D as well as insulation of the trap),

– cool-down of trap and coldhead after desorption (targeted adsorption temperature T_A, cooling capacity, i.e. heat lift around T_A, coldhead insulation and ambient temperature).

Shortening any of these steps can theoretically shorten the overall cycle time, thereby increasing time resolution; however, there might be no benefit in doing so if there are other limitations like the time it takes to record the chromatogram of a sample injection. To give a practical example, Table 2 demonstrates that very short cycle times of 4.1 min are possible with a decreased preconcentration volume (100 mL instead of 500 mL; requiring a detector that is sensitive enough), a slightly higher T_A (∼ −72 °C) and a faster GC. General measures to increase time resolution would be to increase the preconcentration flow, reduce the sample size (see in situ set-up), improve the coldhead and trap insulation and increase the cooling capacity.

Table 2. Cycle times at T_A of $-80\,°C/-120\,°C$ (laboratory set-up) and $-70\,°C$ (in situ set-up), based on operational data. Laboratory set-up configuration: Sunpower CryoTel CT Stirling cooler, preconcentration volume: 500 mL at 100 mL min^{-1}, $T_D \approx 200\,°C$ for 3 min. In situ set-up configuration: Twinbird SC-TD08 Stirling cooler with preconcentration volume of 100 mL at 100 mL min^{-1}, $T_D \approx 200\,°C$ for 1 min. Adsorptive material in both set-ups was HayeSep D. Due to a smaller coldhead, cooling rate and warm-up during desorption are considerably larger with the in situ set-up, despite the shorter desorption time.

T_A [°C]	Cooling rate at T_A [°C min^{-1}]	Warm-up during desorption [°C]	Minimum preconcentration cycle time [min]	Experimental total time needed for one measurement [min]
		Laboratory instrument (GC-TOFMS)		
−80	−2.2	7.7	8.5	19.6
−120	−1.2	16.3	18.6	19.6
		In situ instrument (GhOST-MS)		
−70	−4.1	13.5	4.1	4.1

After desorption, temperature of the trap drops in an exponential-decay-shaped curve due to the decreasing temperature difference ΔT between coldhead and trap. After a desorption at $T_D \approx 200\,°C$, preconcentration trap and coldhead temperature reach similar temperatures after approximately 30 s cool-down time ($T_A,= -80\,°C$). This time increases to about 90 s at $-120\,°C$ coldhead temperature until ΔT reaches approximately zero. Considering the total run times shown in Table 2, trap cool-down to coldhead temperature is not a limiting factor to the overall cycle time. Consequently, thermal insulation of the trap could still be increased, thereby decreasing coldhead warm-up during desorption.

2.3 Thermodesorption: preconcentration trap heater

Depending on the targeted substance class to analyse and the analytical technique, the requirements for thermodesorption will differ. In the case of a gas chromatographic system for analysis of volatile compounds, these requirements are as follows:

– a fast initial increase in temperature to yield a sharp injection of highly volatile analytes onto the GC column,

– no overshooting of a maximum temperature in case of thermally unstable sample compounds or adsorptive material (e.g. HayeSep D, $T_D < 290\,°C$),

– preservation of the desorption temperature over a time period for desorption of analytes with higher boiling points,

– good overall repeatability, especially of the injection of highly volatile analytes.

Desorption heating is implemented by pulsing a direct current (max. 12 V / 40 A, relay: Celduk Okpac; spec. switching frequency 1 kHz, Celduk Relays, France) directly through
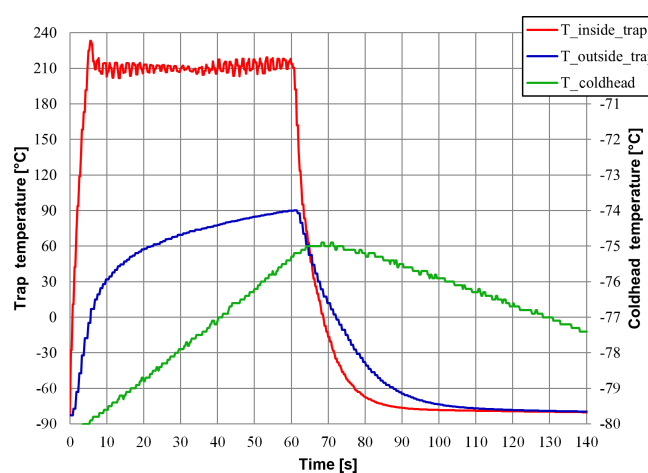

Figure 3. Desorption temperature curve inside the dummy trap (empty tube) with a preceding adsorption temperature of $-80\,°C$ and a subsequent cool-down from desorption to adsorption temperature. Left y axis: red curve represents T_inside_trap, the signal from temperature sensor shifted inside the trap; blue curve represents T_outside_trap, the temperature sensor signal from the sensor welded to the outer trap tubing wall. Right y axis: green curve represents T_coldhead, the temperature of the coldhead. Deterministic heater output in this example is 50 % in stage 1, held for 5 s, and 30 % in stage 2, held for 55 s. The periodic oscillation of T_D observed is a result of a very slow pulse-width modulation used in the testing set-up: 100 ms period with 10 ms minimum increment.

the trap tubing which has a resistance of $\sim 0.5\,\Omega$. A temperature sensor (Pt100, 1.5 mm OD) was welded to the outside of the trap tubing (see also Fig. 2), for feedback control of the heater temperature. However, mainly due to the thermal mass of the sensor and its proximity to the coldhead (despite the insulation), it was found to give no representative values for temperature inside the trap during desorption. Differences of around $100\,°C$ were found in comparison to tem-

perature measured within the trap (equilibrium state reached after 2–3 min of continuous heating). Nevertheless, the temperature sensor can (after being characterised) be used for feedback control as the indicated values are reproducible. As an alternative to feedback control, a deterministic heater with prescribed output settings can be used. For security reasons, measured coldhead and trap temperature have to be used as heater shutdown triggers in this case.

Figure 3 shows a comparison of temperature sensor data from in- and outside the empty trap as well as the coldhead. Very good results were achieved with a two-stage, deterministic heater set-up with a fast warm-up (stage 1), a small over-shoot of T_D and preservation of T_D (stage 2) with only a small drift and fluctuation. With the described heater set-up, T_D can be reached within a very short time of approximately 3 s. Initial heating rates (first second of heat pulse) were calculated to be more than $200\,°C\,s^{-1}$ depending on the power output setting. As the trap warms, heating rate drops, resulting in a mean heating rate of about $80\,°C\,s^{-1}$ during stage 1.

If a deterministic heater is used instead of a feedback controlled heater, the temperature of the trap becomes directly dependent on coldhead temperature (more precisely, heat flows from the trap into the coldhead). Consequently, higher output settings are necessary at lower coldhead temperatures to achieve comparable temperatures. On the other hand, if the coldhead gets warmer, trap temperature increases as well. This effect can be observed in Fig. 3 as a slight upward drift of the trap temperature (red curve, temperature measured within the trap) during stage 2. The absolute temperature differences caused by this drift as well as the oscillation amplitude are small (in Fig. 3: approximately $20\,°C$ min. to max. and $4\,°C$ standard deviation without trend correction) compared to the temperature difference between coldhead and trap during heating ($\sim 300\,°C$). An effect of this temperature oscillation during desorption on gas flow through the adsorptive material (and thereby on injection) cannot be excluded. However, our experience with different heater set-ups (feedback controlled and deterministic, with different pulse-width modulation periods) suggests that it plays a minor role at most for the actual trap, at least in terms of overall measurement repeatability.

Besides the problem of differing inner and outer temperature of the trap during heating, temperature was not found to be distributed homogeneously alongside the empty trap inside the coldhead. Temperature differences of up to $\pm 30\,°C$ at a mean temperature of $200\,°C$ were observed with the current set-up when measuring temperature at different points within the trap. These values are potentially afflicted by poor accuracy due to difficulties in measuring the inner temperature (wall contact of sensor). Potential causes for the temperature differences are inhomogeneity in trap insulation as well as variations in tubing wall width or carbon content leading to an inhomogeneous electrical resistance and thus an inhomogeneous distribution of heat. These temperature variations might be different or ideally negligible in the actual precon-

centration trap. However, the finding underlines the importance of insulation being as homogeneous as possible and suggests that cold points (potentially insufficient desorption) as well as hot points (potentially adsorptive material / analyte decomposition) can occur along the trap. This has to be taken into consideration when setting up and testing the preconcentration set-up, i.e. to not exceed the temperature limit of the adsorptive material.

3 Performance characteristics

This section discusses characterisation results (Sect. 3.2 and 3.3) obtained with the GC-TOFMS instrument described in Obersteiner et al. (2016) as it covers the widest range of substances (see Supplement) and, therefore, allows for the most differentiated analysis. A brief description of this analytical instrument is given in the following Sect. 3.1; see Obersteiner et al. (2016) for details on GC and MS. We consider these results to also be valid in principle for our other GC–MS set-up discussed by Hoker et al. (2015) and the GhOST-MS described by Sala et al. (2014) as all preconcentration set-ups rely on the same principal set-up and similar components are used (see Table 1). Please refer to the relevant publications for the discussion of instrument characteristics, e.g. measurement precision or reproducibility which are not exclusively related to the preconcentration set-up.

3.1 Analytical instrument

A Sunpower CryoTel CT free piston Stirling cooler (Ametek Inc., USA) is used for cooling the coldhead. In the described set-up, a water coolant system (Alphacool, Germany), originally intended for cooling computer processing units, removes heat from the Stirling cooler's heat rejection. Sunpower Stirling coolers are also optionally available with an air-fin heat rejection which require a continuous airstream during operation. To control the heater of the trap, a pulse-width modulation (PWM; 20 ms period, 1 µs minimum width) with a prescribed output is used (deterministic heater; see Sect. 2.3). Heater operation during desorption is separated into a short initial warm-up stage with a high output of the PWM and a longer hold stage with lower heater output to maintain desorption temperature. The trap is packed with adsorptive material over a length of approximately 100 mm (~ 20 mg). Two different adsorptive materials were used in different traps installed over the course of this work: HayeSep D, 80/100 mesh (VICI International AG, Switzerland) and Unibeads 1S, 60/80 mesh (Grace, USA).

A Bronkhorst EL-FLOW F-201CM (Bronkhorst, the Netherlands) is used for sample flow control (downstream of the trap in order to avoid contamination) in combination with a Baratron 626 pressure sensor (0–1000 mbar, accuracy incl. non-linearity 0.25 % of reading, MKS Instruments, Germany) for analyte quantification by pressure difference mea-

surement. An Agilent 7890 B gas chromatograph (GC) with a GS GasPro PLOT column (Agilent Technologies, Inc. USA; 0.32 mm inner diameter) using a ramped temperature programme (45 to 200 °C with 25 °C min^{-1}) and backflush option is used for analyte separation. Purified helium 6.0 is used as carrier gas (Praxair Technologies Inc., German supplier; purification system: Vici Valco HP2). For analyte detection, a Tofwerk EI-TOF (model EI-003, Tofwerk AG, Switzerland) mass spectrometer is attached to the GC. All samples are dried using magnesium perchlorate kept at 80 °C prior to preconcentration. Artificial additions of analytes to the sample from the dryer were excluded by comparing measurements of dried and undried blank gas. All tubing upstream of the trap was heated to > 100 °C to avoid substance loss to tubing walls.

Two different adsorptive materials were used in the course of this work (HayeSep D, Unibeads 1S) which showed partly differing adsorption and desorption properties. The results are discussed separately where appropriate in Sect. 3.3.1 and 3.3.2). To achieve high measurement precision and minimum uncertainties introduced by the preconcentration unit, both the analyte adsorption (preconcentration) and analyte desorption (injection) into the chromatographic system have to be quantitative and repeatable. The following section describes tests and results for the characterisation of both aspects.

3.2   Adsorption

The preconcentration trap is essentially a micro-packed chromatographic column with a limited surface area where sorption can take place. The low temperature during sample preconcentration shifts the steady state of analyte partitioning between mobile and solid phase, mostly to the solid phase. With this preconcentration technique, the most abundant constituents of the air (nitrogen, oxygen and argon) are mostly removed from the sample. Other, less volatile but still very abundant constituents like CO_2 are, however, trapped, depending on adsorption temperature. Elution of such species from the GC column after thermodesorption and injection can cause problems with regard to chromatography (e.g. peak tailing) as well as detection (e.g. detector saturation), depending on GC configuration and detection technique. With the set-up described, the elution of CO_2 limits the analysable substance range as the detector shows saturation during the elution of CO_2 (ionisation switched off until tolerable CO_2 levels are reached). A CO_2 removal technique could, therefore, improve chromatographic performance and extend the substance range of the current preconcentration system. At lower adsorption temperatures, even with CO_2 removal, a similar problem could, however, be caused by other gases, e.g. xenon (boiling point: −108 °C), which is still more abundant by 3 orders of magnitude in the atmosphere than the analytes discussed here. Interactions of other, reactive species

like ozone with analytes (e.g. alkenes) during trapping and desorption were not investigated in this work.

Regarding preconcentration of targeted analytes, the concept of an adsorption–desorption steady state suggests that at a certain point a breakthrough of analytes occurs, depending on a combination of loading the solid phase with sample molecules and the time to achieve steady state, in turn influenced by sample flow rate and pressure. Consequently, the maximum possible sample volume and/or minimum duration of preconcentration are dependent on the adsorptive material used, volatility (and concentration) of the targeted analytes as well as sample flow rate and pressure. For typical sample volumes of 0.5 and 1.0 L (at standard temperature and pressure) and a constant sample back pressure of 2.5 bar abs. (back pressure indicated by the regulator of the sample flask), no significant impact of sample preconcentration flow was found within the tested range of 50 to 150 mL min^{-1} for any of the analysed substances. Higher or lower flow rates and pressure were not possible or suitable for practical reasons like flow restriction and valve operating pressure.

Substance breakthrough (i.e. substance-specific adsorption capacity) was analysed in volume variation experiments, comprising measurements of the same reference air with preconcentration volumes of up to 10 L and referencing the volume-corrected detector response against default preconcentration volumes, e.g. 1 L (relative response). Quantitative trapping is then indicated by a relative response of 100 %; a relative response < 100 % indicates an underestimation (i.e. loss by breakthrough), while a relative response of > 100 % indicates an overestimation (i.e. increase by a memory effect from the preceding sample). To structure the following discussion, two classes of substances are formed and treated separately: medium volatile substances with boiling points > −30 °C (e.g. CFC-12, CCl_2F_2) and highly volatile substances with boiling points < −30 °C (e.g. HFC-23, CHF_3). The substances are selected based on the criteria volatility and (preferably high) concentration. The adsorption of substances with lower volatility (BP > 30 °C) was assumed to be quantitative. Results discussed in the following are displayed in Table 3.

3.2.1   Medium volatile substances

As a reference for halocarbon analysis, CFC-12 (CCl_2F_2) and CFC-11 (CCl_3F) were chosen due to their high mixing ratios of about 525 and 235 pmol mol^{-1} (ppt, parts per trillion) in present-day, ambient air and moderate volatility with boiling points of −29.8 and +23.8 °C. For a volume of 10 L preconcentrated air on the Unibeads 1S trap, both substances showed a deviation from linear response of +0.6 % ± 0.42 % for CFC-12 and +0.6 % ± 0.22 % respectively for CFC-11. The positive deviation from linearity is still found within the 3-fold measurement precision determined for the experiment and could potentially be an artefact of the detector, which tends to slightly overestimate strong signals and underesti-

Table 3. Results from a volume variation experiment, comprising measurements of the same reference air with preconcentration volumes (PrcVol) of up to 2, 5 and 10 L. Laboratory set-up using adsorptive material Unibeads 1S. Volume-corrected detector response is referenced against calibration preconcentration volumes of 1 L (rR). rR < 100 % indicates underestimation (e.g. loss by breakthrough); rR > 100 % indicates overestimation (e.g. increase by a memory effect from the preceding sample or contamination). Breakthrough is observed for COS at a preconcentration volume of 10 L while ethyne shows signs of a system contamination (rR > 100 % despite a higher volatility compared to COS). CFC-12 and CFC-11 show no indication of breakthrough, with all deviations from 100 % rR below 3σ.

Substance	PrcVol [L]	rR	rR: 1σ	PrcVol [L]	rR	rR: 1σ	PrcVol [L]	rR	rR: 1σ
Ethyne (C_2H_2)		102.0 %	0.66 %		108.9 %	0.70 %		109.2 %	0.70 %
Carbonyl sulfide (COS)		102.2 %	0.82 %		100.9 %	0.81 %		64.8 %	0.52 %
CFC-12 (CCl_2F_2)	2	99.9 %	0.41 %	5	100.7 %	0.42 %	10	100.6 %	0.42 %
CFC-11 (CCl_3F)		100.2 %	0.21 %		100.5 %	0.22 %		100.6 %	0.22 %

mate weak signals; see Sect. 3.4 in Obersteiner et al. (2016). Hence, no significant breakthrough or detector saturation was observed for either CFC-12 or CFC-11.

3.2.2 Highly volatile substances

Carbonyl sulfide (COS) is more volatile compared to CFC-12 and CFC-11 but similar in mixing ratio, with a boiling point of $-50.2\,°C$ and an ambient air mixing ratio of around 500 ppt. Against 1 L reference sample volume (sample mixing ratio: 525 ppt), COS showed a quantitative adsorption up to 5 L on the Unibeads 1S trap with a deviation from linear response of $+0.9\,\% \pm 0.80\,\%$. At 10 L sample volume, a breakthrough occurred, giving a deviation from the linear response of $-35.2\,\% \pm 0.52\,\%$. The substance analysed with highest volatility was HFC-23 with a boiling point of $-82.1\,°C$ and a current background air mixing ratio of ~ 40 ppt. Referenced against a sample volume of 0.5 L, significant breakthrough occurred at a sample volume of 2.5 L with a deviation from the linear response of $-39.2\,\% \pm 2.75\,\%$. The highest sample volume quantitatively adsorbed in the experiment was 1.0 L with a relative response of $-0.3\,\% \pm 2.75\,\%$ (HayeSep D trap). A similar behaviour was observed for ethyne (C_2H_2), with a sublimation point of $-80.2\,°C$, a mixing ratio of approximately 610 ppt in the sample and a deviation from linear response of $-20.2\,\% \pm 1.22\,\%$ at 2.5 L sample volume (HayeSep D trap). However, ethyne was also analysed on the Unibeads 1S trap which gave a quite different result with a deviation from linear response of $+10.1\,\% \pm 0.51\,\%$, thus breakthrough is unlikely. The positive, non-linear response is caused potentially by a system blank (see also Sect. 3.3) or non-linear detector response. Unfortunately, HFC-23 could not be analysed in ambient air samples for comparison on the Unibeads 1S trap as its ion signals are masked by large amounts of CO_2 still eluting from the GC column at the retention time of HFC-23.

Concluding, the adsorption process was found to be substance specific as both HFC-23 and ethyne are comparably volatile but significantly less ethyne broke through despite its 15-fold elevated mixing ratio (Unibeads 1S trap). The comparison of ethyne breakthrough on the HayeSep D and Unibeads 1S trap suggests that the adsorption process is dependent on the chosen adsorptive material. A comparison of adsorptive materials is, however, not the focus of this work. Such a comparative adsorption study was conducted for methane (CH_4) preconcentration by Eyer et al. (2014), for example. From the comparison of the breakthrough observed for COS and the quantitative adsorption of CFC-12 and CFC-11, it can be concluded that volatility is the primary factor that determines breakthrough. Quantitative adsorption is not limited by principal adsorption capacity (i.e. the absolute number of molecules adsorbed) of the adsorptive material and material amount for a sample volume of up to 10 L and an adsorption temperature of $-80\,°C$.

3.3 Desorption

While adsorption is characterised by the quantitative trapping of highly volatile substances, desorption is characterised by sharpness and repeatability of the injection represented by chromatographic peak shape and retention time variance during a measurement series (Sect. 3.3.1). Additionally, the appearance and quantity of analyte signals in measurements of an analyte-free gas after sample measurements determine the number of analysable substances and, ultimately, measurement data quality. The discussion of analyte residues can be found in Sect. 3.3.2. Figure 4 shows a typical chromatogram recorded after desorption and injection of a preconcentrated ambient air sample for three selected mass-to-charge ratios (m/Q).

Table 4. Retention times t_R with relative standard deviations rSD and variances for selected substances (same as Table 3) as well as their respective average signal width expressed as FWHM. Values derived as arithmetic means over four measurement series from different dates (April 2015 to June 2016), comprising 149 individual measurements ($\sim$ 37 per series) of 19 different ambient air samples using the ramped GC programme. For retention time variance, maximum to minimum differences over the four measurement series are given in brackets. Trap adsorptive material: HayeSep D. HFC-23 is the first detectable substance, least separated by chromatography. CFC-11 can be considered a reference for optimal chromatographic performance of the given set-up.

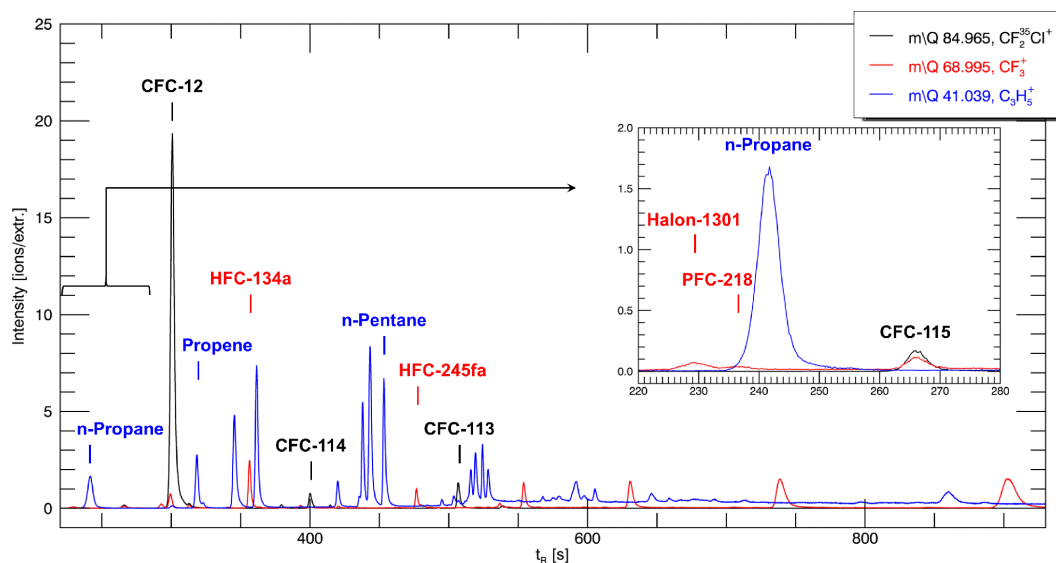| Substance	t_R [min]	t_R rSD	Variance [s^2]		Peak width [s]
HFC-23 (CHF$_3$)	3.01	0.107 %	0.042	(0.0440)	4.235
Ethyne (C$_2$H$_2$)	3.74	0.045 %	0.011	(0.0111)	2.773
Carbonyl sulfide (COS)	3.86	0.039 %	0.009	(0.0145)	2.674
CFC-12 (CCl$_2$F$_2$)	5.01	0.039 %	0.009	(0.0093)	2.457
CFC-11 (CCl$_3$F)	7.25	0.016 %	0.003	(0.0050)	2.462

Figure 4. Chromatogram from a 1 L ambient air sample obtained with the GC–MS set-up described in Obersteiner et al. (2016). X axis: retention time t_R in seconds. Y axis: signal intensity expressed as ions per extraction which are derived from a 22.7 kHz TOFMS extraction rate, averaged to yield a mass spectra rate of 4 Hz. X and y axis descriptions are also valid for the magnified section. Black graph: mass-to-charge ratio $(m/Q) = 84.965$ signal from a typical CFC fragment ion $CF_2^{35}Cl^+$. Red graph: $m/Q = 68.995$ signal from a typical PFC or HFC fragment ion CF_3^+. Blue graph: $m/Q =$ 41.039 signal from a typical hydrocarbon fragment ion $C_3H_5^+$. The magnified section shows the chromatographic peak of propane and three other compounds to demonstrate injection quality of substances least refocused by chromatography.

3.3.1 Peak shape and retention time stability

To demonstrate injection sharpness, Fig. 5a shows the chromatographic signal of CFC-11 eluted from the GC column kept isothermal at 150 °C and Fig. 5b the chromatographic signal as observed with the ramped GC programme. Both signals generally show a Gaussian peak shape with a slight peak tailing. In comparison, the unfocused signal from the isothermal column reflecting the sharpness of the direct injection is wider by a factor of $\sim$ 3 but still narrow enough to allow for good peak separation in most standard GC methods with runtimes between 10 to 30 min. The full peak width at half maximum (FWHM) was calculated to be 6.3 s (0.10 min)

for the isothermal peak and 2.0 s (0.03 min) for the focused peak.

Injection quality can be further judged by the stability of retention times of the first chromatographic signals obtained with the ramped GC programme, as these are only very slightly influenced by the chromatographic system (see also Fig. 4). In particular, there is nearly no refocusing on the chromatographic column. Table 4 shows retention times and their variability expressed as relative standard deviation and variance as well as the chromatographic signal width (FWHM) of the respective substance. Four measurement series were investigated, comprising 149 individual measurement and 19 different ambient air samples. Variances are less
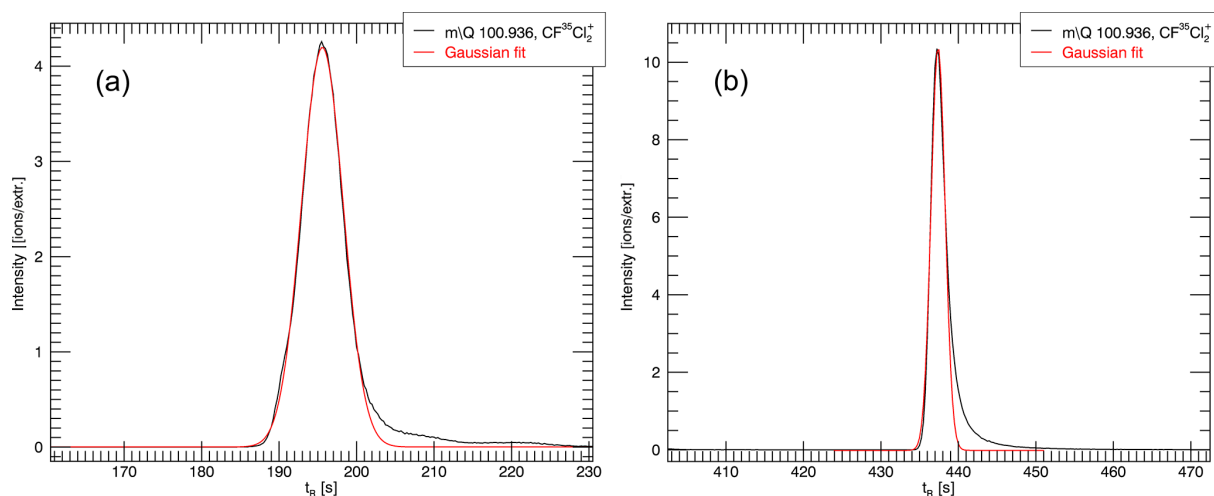
Figure 5. Comparison of chromatographic peak shapes of the $CF^{35}Cl_2^+$ fragment ion signal of CFC-11 ($CFCl_3$) from an injection of 1 L preconcentrated ambient air onto the GC column kept isothermal at 150 °C **(a)** and onto the GC column kept at 45 °C and ramped to 200 °C subsequently (**b**; see Sect. 3.1). X axis: retention time t_R in seconds; t_R interval shown is 70 s in both plots. Y axis: signal intensity expressed as ions per extraction (see Fig. 4). The red curve shows a Gaussian fit for comparison of actual peak shape and a peak shape that is considered ideal. FWHM of fit: **(a)** 6.3 s (0.10 min) and **(b)** 2.0 s (0.03 min). Adsorptive material: Unibeads 1S.

than $0.02\,s^2$ on average. Together with signal width, they decrease inversely proportional to retention time, which shows the increasing influence of chromatographic separation (from HFC-23 to CFC-11 in Table 4). Even at incomplete refocusing by gas chromatography, the desorption procedure of the preconcentration unit gives close to Gaussian peak shapes except a slight tailing. Parts of this tailing effect, which originates from desorption, could potentially be reduced by refocusing the high-volatile analyte fraction on a second trap (e.g. Miller et al., 2008). The high repeatability of the injection is shown by the low variability in retention time of the first signals in the chromatogram (Table 4).

3.3.2 Analyte residues

Analyte residues can represent an inherent system contamination (1) or constitute a remainder from the previous sample (memory effect (2)). Both types of residues can originate from different sources, e.g. the adsorptive material (preconcentration trap), valve membranes. They are differentiated by either an ever-present blank signal (1) or a blank signal that decreases to zero in repeated measurements of an analyte-free zero gas after sample measurements (2).

Analyte residues were investigated with (a) unloaded injections after multiple 1 L ambient air sample injections, i.e. subsequent thermodesorption of the trap without switching to load position between runs (see Fig. 1) and (b) the preconcentration of 1 L helium from the carrier gas supply using the same path as the sample, including dryer, etc. after multiple 1 L ambient air sample measurements. Analyte residues on the trap (preconcentration trap memory or contamination), as well as carrier gas contaminations, are inves-

tigated by (a) while (b) includes analyte residues within the tubing upstream of the trap, stream selection, sample dryer, etc. (system memory or contamination). The differentiation between (a) and (b) allows for a separate investigation, for which memory effect or contamination could potentially be reduced through the choice of adsorptive material or parameters of the desorption process (e.g. T_D) (a) and for which a part has to be attributed to tubing, stream selection, etc. (b).

To get the most complete picture possible, 65 substances were analysed, most of them halo- and hydrocarbons (see Supplement for a detailed list) on both a HayeSep D as well as a Unibeads 1S trap. Substances with low measurement precision (> 10 %) were excluded from the investigation. In general, most of the detected analyte residues are probably caused by system contaminations (HFCs from fittings, solenoid valve membranes, etc.) or carrier gas contaminations (hydrocarbons) as they show a constant background. A distinct attribution of specific sources was not attempted. Please also note that potential contamination sources might be different for different instrumental set-ups, individual sources might disappear over time (aging), etc. Regarding system memory, including the trap, the amount of a residue is dependent on volatility and concentration, so extremely elevated concentrations of low-volatile substances in the previous run might lead to a memory effect that was not detected in the current investigation with 1 L preconcentration volume of unpolluted ambient air. Detailed results for the two different adsorptive materials tested are discussed in the following.
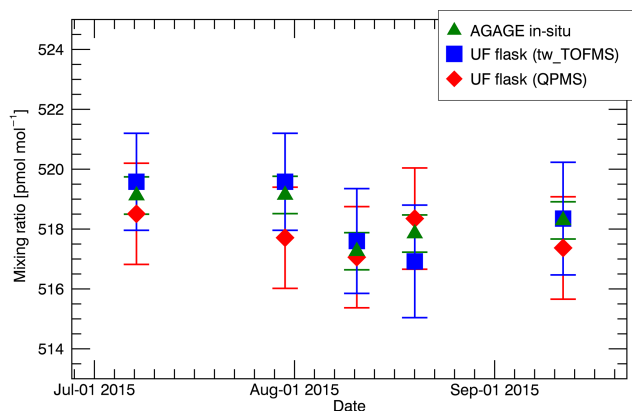
Figure 6. CFC-12 (CCl_2F_2) mixing ratios at Mace Head Atmospheric Research Station, Ireland ($53°20'°$ N, $9°54'°$ W, 30 m above sea level) derived from 2 L stainless steel flask samples measured with our GC-TOFMS (blue squares), our reference instrument (GC-QPMS, red diamonds) and values taken from the online measurement data of the in situ Medusa GC–MS (green triangles). Error bars are 1-fold the measurement precision of each instrument (Medusa system: typical precision taken from Miller et al., 2008). Calibration scale of all instruments: SIO-05.

Unibeads 1S adsorptive material

Out of 65 substances, 13 (20 %) showed detectable residues on the trap which did not represent a system memory but a system contamination from the carrier gas, sealing materials, etc. as they were always present and did not disappear in subsequent unloaded injections. Respective residues were generally larger with increasing boiling point (e.g. propane < benzene). Most of them were hydrocarbons and the halocarbons chloro- and iodomethane (CH_3Cl, CH_3I) and chloroethane (C_2H_5Cl) as well as HFC-134 (CHF_2CHF_2). No further CFCs, HCFCs, PFCs or HFCs were detected in the unloaded trap injection (see Obersteiner et al., 2016 for a discussion of detection limits). Of the remaining 52 substances, 36 also did not show any detectable residues in the helium blank. Of the 17 substances that did show residues (contamination and memory effect combined), 7 had residues below 0.5 % of the signal area determined in the preceding ambient air measurement. Again, residues were found mostly for hydrocarbons but not CFCs or HCFCs. Concluding, the Unibeads 1S trap seems to be a good choice for halocarbon monitoring measurements (one measurement per sample) as there were nearly no halocarbon residues in subsequent helium blank measurements.

HayeSep D adsorptive material

The HayeSep D trap showed a considerably higher amount of preconcentration trap residues (unloaded injection) with 22 detectable substances from the selected 65 (34 %). Again, most of these substances were hydrocarbons but also some

halogenated compounds like Tetrachloromethane (CCl_4) and Bromoform ($CHBr_3$). Of the remaining 43 substances, 28 were undetectable in the helium blank (system free of contamination or memory effect). Thirteen of the detectable substances showed responses of < 0.5 % relative to the preceding ambient air sample, including CFC-11 with 0.05 % and CFC-113 with 0.2 %. While the named halogenated compounds CCl_4 and $CHBr_3$, as well as CFC-113 and CFC-11, were undetectable in subsequent blank gas measurements, residues of many hydrocarbons were persistent, suggesting a system contamination. In summary, the HayeSep D trap showed an overall higher number of residues, likely caused by a higher desorption temperature of the Unibeads 1S trap which can be heated faster and to a higher temperature without degrading the material. Nevertheless, the residues on both adsorptive materials were on a tolerable level (below average measurement precision) for flask measurements with multiple measurements per sample.

4 Application

4.1 Laboratory operation: flask sample measurements

To ensure internal consistency of our laboratory instrumentation, five air samples were analysed with the GC-TOFMS instrument (Obersteiner et al., 2016) and compared to our reference GC-QPMS (gas chromatograph coupled to a quadrupole mass spectrometer) which uses a similar preconcentration set-up (Hoker et al., 2015). Consistent results with the NOAA network (National Oceanic and Atmospheric Administration) have been demonstrated for the GC-QPMS in the past during the international halocarbons in air comparison experiment (IHALACE; Hall et al., 2014) intercomparison (Hall et al., 2014), but with a different sample preconcentration using liquid nitrogen (Brinckmann et al., 2012; Laube and Engel, 2008; Laube et al., 2010). The current laboratory set-up using the Stirling cooler-based preconcentration has been described by Hoker et al. (2015) and has shown very consistent results with previous measurements. The samples for the application and intercomparison discussed here were collected between 7 July and 11 September 2015 at Mace Head Atmospheric Research Station in Ireland ($53°20'°$ N, $9°54'°$ W, 30 m above sea level). Samples were filled "moist" (no sample drying) into 2 L electro-polished stainless steel flasks (two flasks in parallel per sampling date). To test the overall performance, the comparison is extended to include in situ measurement data from the online monitoring Medusa GC–MS (Miller et al., 2008) operated by the AGAGE (Advanced Global Atmospheric Gases Experiment) network at Mace Head Station. Medusa GC–MS data points were chosen within ±1 h of the flask samples' sampling time. Figure 6 shows a comparison of absolute quantification results for CFC-12 (CCl_2F_2). Very good agreement within the 1-fold measurement error is achieved in comparison to the Medusa
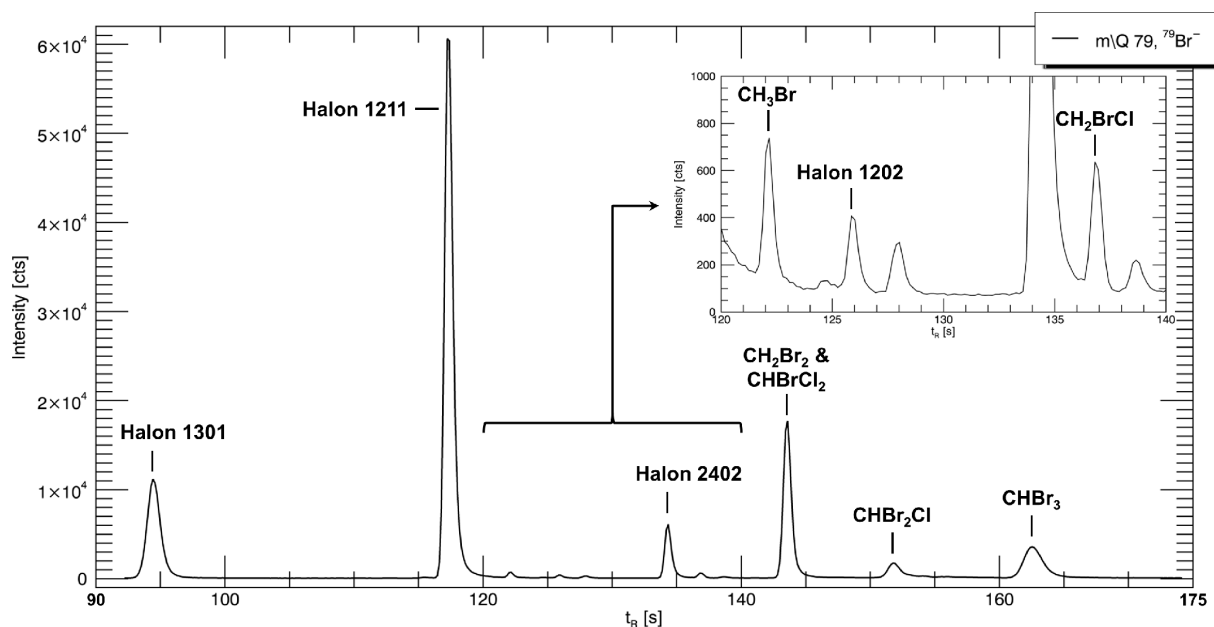
Figure 7. Chromatogram from a preconcentration of 0.1 L ambient air obtained with the in situ GC–MS set-up GhOST-MS. X axis: retention time t_R in seconds. Y axis: signal intensity in counts, arbitrary unit. MS: Agilent 5975C in negative chemical ionisation mode (reagent: argon). Black graph: mass-to-charge ratio $m/Q = 79$ signal of $^{79}Br^-$ ions from brominated trace gases.
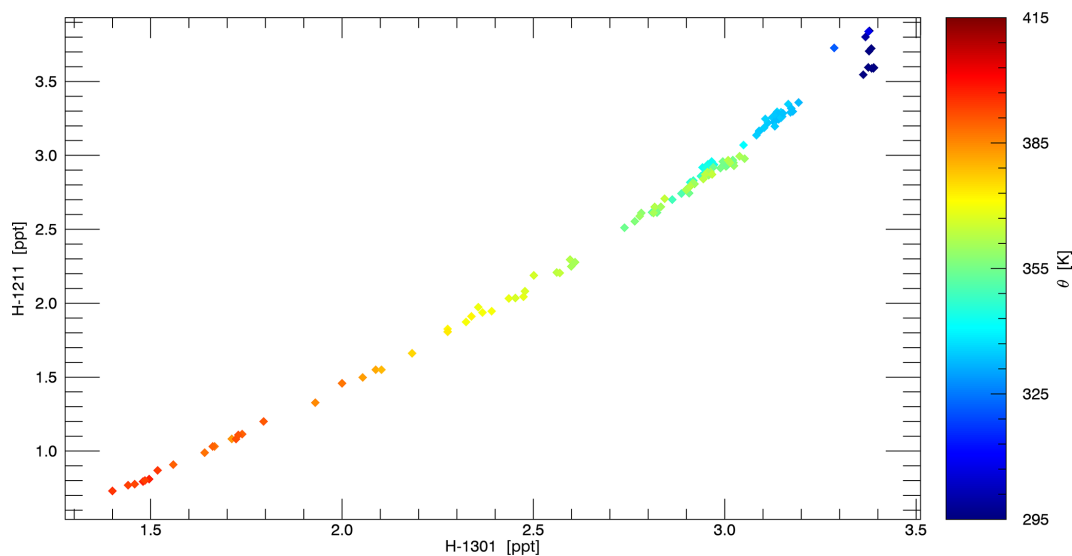

Figure 8. Tracer–tracer correlation of Halon 1301 (CBrF$_3$, x axis) vs. Halon 1211 (CBrClF$_2$, y axis). Colour code indicates potential temperature θ in [K]. Data were obtained during the POLSTRACC mission with the HALO aircraft, flight 160226a (PGS-14). Preliminary data. Calibration scale of Halon 1301 and 1211: SIO-05. Preliminary measurement precision and calibration uncertainty: 0.4 %/1.7 % (Halon 1301), 0.2 %/0.9 % (Halon 1211).

GC–MS and within the 2-fold measurement error in comparison to the reference GC-QPMS. While the Medusa GC–MS is calibrated with secondary calibration gases (AGAGE flasks H-265 and H-266; CFC-12 scale: SIO-05), both our instruments were calibrated with different ternary calibration gasses, referenced to the same secondary calibration gas (AGAGE flask H-218; CFC-12 scale: SIO-05). Taking into account that all three instruments were calibrated with different calibration gases which rely on the same calibration scale but are based on a chain of intercalibrations, this result is proof for highly accurate measurement results, excluding the absolute scale error.

4.2 Aircraft in situ operation: GhOST-MS

Reliability of operation is best demonstrated with the in situ GC–MS GhOST-MS. Figure 7 shows a chromatogram obtained from the injection of a preconcentrated sample volume of 100 mL of ambient air. With a chromatographic runtime of 2.9 min and a total cycle time of 4.1 min (see also Table 2), a data frequency is achieved that is very high for a GC–MS system with a total of 27 identified and simultaneously measured species on m/Q of bromine, chlorine and iodine in negative chemical ionisation mode using argon as reagent gas. The cycle time is limited by cool-down of the adsorptive material (HayeSep D) to $-70\,°C$ needed to quantitatively trap the earliest eluting analyte, Halon 1301 ($CBrF_3$). The very good overall performance of the GhOST-MS including the preconcentration unit used in this in situ application can be inferred from actual measurement data obtained during a research flight of the recent PGS campaign (POLSTRACC/GW-LCycle/SALSA) of the HALO aircraft on flight 160226a (PGS-14). Figure 8 shows a tracer–tracer correlation between Halon 1301 and Halon 1211 ($CBrClF_2$). The measurements are colour-coded to show potential temperature θ. As expected, the lowest mixing ratios are observed at the highest potential temperature. Both tracers have relatively long steady-state lifetimes of 72 years for Halon 1301 (58–97, derived from model data and observations) and 16 years for Halon 1211 (10–39, model data) (SPARC, 2013) so that a compact correlation of mixing ratios of these two traces gases is expected in the stratosphere (Plumb and Ko, 1992). Due to its relatively low boiling point ($-57.8\,°C$), Halon 1301 is the first species eluting from the chromatographic column. The shape of the chromatographic peak is thus strongly influenced by the injection, as refocusing on the chromatographic column is expected to play a negligible role. As a correlation derived from measurement data can only be as compact as the measurement precision allows, the compactness of the correlation shown in Fig. 8 gives an indication of the high measurement precision achieved with the GhOST-MS. The fact that this compact correlation includes a substance with a precision that is strongly influenced by its thermodesorption shows that the sample preconcentration system on GhOST-MS is able to reproducibly trap and desorb even low-boiling compounds like Halon 1301.

GhOST-MS has been deployed during a total of more than 200 flight hours on the HALO aircraft without a single failure of the preconcentration unit. In addition, measurements with GhOST-MS were performed as part of the SHIVA campaign in Borneo, providing a complete bromine budget for the upper tropical troposphere up to about 13 km (Sala et al., 2014). The preconcentration unit presented here, therefore, is not only able to provide high precision but is also able to operate reliably under difficult conditions like aircraft operation with varying humidity and temperatures, including operation during humid and hot conditions in the tropics.

5 Summary and conclusion

A single-stage, refrigerant- and cryogen-free sample preconcentration unit for ambient air analysis is presented and characterised. The set-up has proven to be applicable for both in situ and laboratory operation and can quantitatively trap and desorb a wide range of halogenated trace gases and potentially also hydrocarbons (see Supplement). The use of different adsorptive materials is possible with the set-up, two of which were used during this work, HayeSep D and Unibeads 1S. Both materials are well suited for analysing halogenated trace gases in general. While HayeSep D is an established material for this task, Unibeads 1S is potentially a good alternative, showing better heat tolerance and fewer analyte residues in the presented characterisation.

The preconcentration unit is positioned between more sophisticated but also more expensive and complicated solutions, e.g. the Medusa preconcentration unit described by Miller et al. (2008) and set-ups that use less powerful, Peltier-based cooling options which sacrifice adsorption temperature, therefore reducing the trappable substance range. The described set-up is unique in terms of the used cooling technique, a Stirling cooler. The latter allows for very low temperatures of $-120\,°C$ tested in this work and $-173\,°C$ reported by Eyer et al. (2016) for the preconcentration of methane with a comparable Stirling cooler without having to rely on a cooling agent like liquid nitrogen or liquid argon. The Stirling cooler as a cooling option is ideally suited for in situ, remote-site operation, where cryogen-based cooling options are very difficult to operate and space is limited – like the aircraft-based in situ GC–MS instrument GhOST-MS. Moreover, the absence of mechanical/moving parts as well as the lack of necessity of vacuum insulation of cooled parts facilitates installation and maintenance. No exchange of adsorption tubes is necessary. Overall, the set-up is relatively cheap with the Stirling cooler being the most expensive part by far.

The simplicity of the single-stage design also has a downside; a major problem is the trapping of large amounts of CO_2 and injection into the detection system (see also Sect. 3.2), especially when using trapping temperatures below $-80\,°C$. Depending on GC and the detection system, this could induce artefacts in the detected signals and, also due to this limitation, the current configuration is not applicable to highly volatile compounds like CF_4, C_2F_6 or C_2H_6. Cooling capacity should, however, be sufficient to ensure quantitative trapping of such compounds on a suitable adsorptive material. Therefore, a starting point for future improvement is removing CO_2 to extend the already large substance range by compounds of higher volatility. Regarding desorption, no blank residues were found for halocarbons which would cause concern or render the set-up unsuited for halocarbon analysis (see Supplement: Blank Residues). Relatively large amounts of hydrocarbons remained in blank measurements. These residues are not an inherent problem of the precon-

centration set-up but more likely due to the adsorptive materials, carrier gas or valve membrane materials. We do not attempt to present a viable correction method for any of the encountered analyte residues here. More dedicated experiments are necessary to account for analyte-specific memory effect and/or contaminations, e.g. by modelling the carry-over from one sample to another and subtracting contamination background. By doing so, the applicability of the preconcentration unit can potentially be extended to quantitative hydrocarbon analysis.

6 Data availability

AGAGE in situ data is made available by the Advanced Global Atmospheric Gases Experiment (AGAGE) network and the Carbon Dioxide Information and Analysis Center (CDIAC) and can be accessed online at http://agage.eas. gatech.edu/data_archive/ (AGAGE, 2016).

Data from the POLSTRACC mission (PGS campaign) are available in the HALO database, but only to mission members. GhOST-MS data can be made available to the reader upon request.

The Supplement related to this article is available online at doi:10.5194/amt-9-5265-2016-supplement.

References

AGAGE: Advanced Global Atmospheric Gases Experiment (AGAGE) network, available at: http://agage.eas.gatech.edu/data_archive/, last access: 25 October 2016.

Apel, E. C., Hills, A. J., Lueb, R. A., Zindel, S., Eisele, S., and Riemer, D. D.: A fast-GC/MS system to measure C_2 to C_4 carbonyls and methanol aboard aircraft, J. Geophys. Res., 108, D20, doi:10.1029/2002jd003199, 2003.

Aragón, P., Atienza, J., and Climent, M. D.: Analysis of organic compounds in air: A review, Crit. Rev. Anal. Chem., 30, 121–151, doi:10.1080/10408340091164207, 2000.

Brinckmann, S., Engel, A., Bönisch, H., Quack, B., and Atlas, E.: Short-lived brominated hydrocarbons – observations in the source regions and the tropical tropopause layer, Atmos. Chem. Phys., 12, 1213–1228, doi:10.5194/acp-12-1213-2012, 2012.

de Blas, M., Navazo, M., Alonso, L., Durana, N., and Iza, J.: Automatic on-line monitoring of atmospheric volatile organic compounds: Gas chromatography-mass spectrometry and gas chromatography-flame ionization detection as complementary systems, Sci. Total Environ., 409, 5459–5469, doi:10.1016/j.scitotenv.2011.08.072, 2011.

Demeestere, K., Dewulf, J., De Witte, B., and Van Langenhove, H.: Sample preparation for the analysis of volatile organic compounds in air and water matrices, J. Chromatogr. A, 1153, 130–144, doi:10.1016/j.chroma.2007.01.012, 2007.

Dettmer, K. and Engewald, W.: Ambient air analysis of volatile organic compounds using adsorptive enrichment, Chromatographia, 57, S339–S347, doi:10.1007/BF02492126, 2003.

Eyer, S., Stadie, N. P., Borgschulte, A., Emmenegger, L., and Mohn, J.: Methane preconcentration by adsorption: A methodology for materials and conditions selection, Adsorption, 20, 657–666, doi:10.1007/s10450-014-9609-9, 2014.

Eyer, S., Tuzson, B., Popa, M. E., van der Veen, C., Röckmann, T., Rothe, M., Brand, W. A., Fisher, R., Lowry, D., Nisbet, E. G., Brennwald, M. S., Harris, E., Zellweger, C., Emmenegger, L., Fischer, H., and Mohn, J.: Real-time analysis of δ^{13}C- and δD-CH_4 in ambient air with laser spectroscopy: method development and first intercomparison results, Atmos. Meas. Tech., 9, 263–280, doi:10.5194/amt-9-263-2016, 2016.

Farman, J. C., Gardiner, B. G., and Shanklin, J. D.: Large losses of total ozone in Antarctica reveal seasonal ClO_x / NO_x interaction, Nature, 315, 207–210, doi:10.1038/315207a0, 1985.

Farwell, S. O., Gluck, S. J., Bamesberger, W. L., Schutte, T. M., and Adams, D. F.: Determination of sulfur-containing gases by a deactivated cryogenic enrichment and capillary gas chromatographic system, Anal. Chem., 51, 609–615, doi:10.1021/ac50042a007, 1979.

Haagen-Smit, A. J. and Fox, M. M.: Ozone formation in photochemical oxidation of organic substances, Ind. Eng. Chem., 48, 1484–1487, doi:10.1021/ie50525a044, 1956.

Hall, B. D., Engel, A., Mühle, J., Elkins, J. W., Artuso, F., Atlas, E., Aydin, M., Blake, D., Brunke, E. G., Chiavarini, S., Fraser, P. J., Happell, J., Krummel, P. B., Levin, I., Loewenstein, M., Maione, M., Montzka, S. A., O'Doherty, S., Reimann, S., Rhoderick, G., Saltzman, E. S., Scheel, H. E., Steele, L. P., Vollmer, M. K., Weiss, R. F., Worthy, D., and Yokouchi, Y.: Results from the international halocarbons in air comparison experiment (IHALACE), Atmos. Meas. Tech., 7, 469–490, doi:10.5194/amt-7-469-2014, 2014.

Helmig, D. and Greenberg, J. P.: Automated in situ gas chromatographic-mass spectrometric analysis of ppt level volatile organic trace gases using multistage solid-adsorbent trapping, J. Chromatogr. A, 677, 123–132, doi:10.1016/0021-9673(94)80551-2, 1994.

Hodnebrog, Ø., Etminan, M., Fuglestvedt, J. S., Marston, G., Myhre, G., Nielsen, C. J., Shine, K. P., and Wallington, T. J.: Global warming potentials and radiative efficiencies of halocarbons and related compounds: A comprehensive review, Rev. Geophys., 51, 300–378, doi:10.1002/rog.20013, 2013.

Hoker, J., Obersteiner, F., Bönisch, H., and Engel, A.: Comparison of GC/time-of-flight MS with GC/quadrupole MS for halocarbon trace gas analysis, Atmos. Meas. Tech., 8, 2195–2206, doi:10.5194/amt-8-2195-2015, 2015.

Hou, Y., Yang, L., Wang, B., Xu, J., Yang, Y., Yang, Y., Cao, Q., and Xie, X.: Analysis of chemical components in tobacco flavors using stir bar sorptive extraction and thermal desorption coupled with gas chromatography-mass spectrometry, Chin. J. Chrom., 24, 601–605, doi:10.1016/S1872-2059(06)60026-6, 2006.

Laube, J. C. and Engel, A.: First atmospheric observations of three chlorofluorocarbons, Atmos. Chem. Phys., 8, 5143–5149, doi:10.5194/acp-8-5143-2008, 2008.

Laube, J. C., Kaiser, J., Sturges, W. T., Bönisch, H., and Engel, A.: Chlorine isotope fractionation in the stratosphere, Science, 329, 1167, doi:10.1126/science.1191809, 2010.

Marenco, A., Gouget, H., Nédélec, P., Pagés, J.-P., and Karcher, F.: Evidence of a long-term increase in tropospheric ozone from pic du midi data series: Consequences: Positive radiative forcing, J. Geophys. Res.-Atmos., 99, 16617–16632, doi:10.1029/94JD00021, 1994.

Miller, B. R., Weiss, R. F., Salameh, P. K., Tanhua, T., Greally, B. R., Mühle, J., and Simmonds, P. G.: Medusa: A sample preconcentration and GC/MS detector system for in situ measurements of atmospheric trace halocarbons, hydrocarbons, and sulfur compounds, Anal. Chem., 80, 1536–1545, doi:10.1021/ac702084k, 2008.

Molina, M. J. and Rowland, F. S.: Stratospheric sink for chlorofluoromethanes: Chlorine atom catalysed destruction of ozone, Nature, 249, 810–812, doi:10.1038/249810a0, 1974.

Monks, P. S., Archibald, A. T., Colette, A., Cooper, O., Coyle, M., Derwent, R., Fowler, D., Granier, C., Law, K. S., Mills, G. E., Stevenson, D. S., Tarasova, O., Thouret, V., von Schneidemesser, E., Sommariva, R., Wild, O., and Williams, M. L.: Tropospheric ozone and its precursors from the urban to the global scale from air quality to short-lived climate forcer, Atmos. Chem. Phys., 15, 8889–8973, doi:10.5194/acp-15-8889-2015, 2015.

Montzka, S. A., Reimann, S., Engel, A., Krüger, K., O'Doherty, S., Sturges, W. T. L. A., Blake, D., Dorf, M., Fraser, P., Froidevaux, L., Jucks, K., Kreher, K., Kurylo, M. J., Mellouki, A., Miller, J., Nielsen, O.-J., Orkin, V. L., Prinn, R. G., Rhew, R., Santee, M. L., Stohl, A., and Verdonik, D. C.: Ozone-depleting substances (ODSs) and related chemicals, Chapter 1 in: Scientific assessment of ozone depletion: 2010, global ozone research and monitoring project report no. 52, World Meteorological Organization (WMO), Geneva, Switzerland, 108 pp., available at: http://www.esrl.noaa.gov/csd/assessments/ozone/2010/report.html (last access: 25 October 2016), 2011.

Obersteiner, F., Bönisch, H., and Engel, A.: An automated gas chromatography time-of-flight mass spectrometry instrument for the quantitative analysis of halocarbons in air, Atmos. Meas. Tech., 9, 179–194, doi:10.5194/amt-9-179-2016, 2016.

O'Doherty, S. J., Simmonds, P. G., and Nickless, G.: Analysis of replacement chlorofluorocarbons using carboxen microtraps for isolation and preconcentration in gas chromatography-mass spectrometry, J. Chromatogr. A, 657, 123–129, doi:10.1016/0021-9673(93)83043-r, 1993.

Plumb, R. A. and Ko, M. K. W.: Interrelationships between mixing ratios of long-lived stratospheric constituents, J. Geophys. Res.-Atmos., 97, 10145–10156, doi:10.1029/92jd00450, 1992.

Saito, T., Yokouchi, Y., Stohl, A., Taguchi, S., and Mukai, H.: Large emissions of perfluorocarbons in east asia deduced from continuous atmospheric measurements, Environ. Sci. Technol., 44, 4089–4095, doi:10.1021/es1001488, 2010.

Sala, S., Bönisch, H., Keber, T., Oram, D. E., Mills, G., and Engel, A.: Deriving an atmospheric budget of total organic bromine using airborne in situ measurements from the western Pacific area during SHIVA, Atmos. Chem. Phys., 14, 6903–6923, doi:10.5194/acp-14-6903-2014, 2014.

Simmonds, P. G., O'Doherty, S., Nickless, G., Sturrock, G. A., Swaby, R., Knight, P., Ricketts, J., Woffendin, G., and Smith, R.: Automated gas chromatograph/mass spectrometer for routine atmospheric field measurements of the CFC replacement compounds, the hydrofluorocarbons and hydrochlorofluorocarbons, Anal. Chem., 67, 717–723, doi:10.1021/ac00100a005, 1995.

Solomon, S.: Stratospheric ozone depletion: A review of concepts and history, Rev. Geophys., 37, 275–316, doi:10.1029/1999rg900008, 1999.

Song, C.-F., Kitamura, Y., Li, S.-H., and Ogasawara, K.: Design of a cryogenic CO_2 capture system based on stirling coolers, Int. J. Greenh. Gas Con., 7, 107–114, doi:10.1016/j.ijggc.2012.01.004, 2012.

SPARC: SPARC Report on the lifetimes of stratospheric ozonedeleting substances, their replacements, and related species, edited by: Ko, M. K. W., Newman P. A., Reimann, S., and Strahan, S. E., SPARC Report No. 6, WCRP-15/2013, available at: www.sparc-climate.org/publications/sparc-reports/ (last access: 25 October 2016), 2013.

Velders, G. J., Fahey, D. W., Daniel, J. S., McFarland, M., and Andersen, S. O.: The large contribution of projected HFC emissions to future climate forcing, P. Natl. Acad. Sci. USA, 106, 10949–10954, doi:10.1073/pnas.0902817106, 2009.